A Microscopic Theory of a Single Hydrogen Centre in Niobium *

K. Hau, P. Frodl, F. Sommer, and F. Wahl
Institut für Theoretische Physik, Universität Tübingen

Z. Naturforsch. **43a**, 914–922 (1988); received August 10, 1988

A microscopic theory of a single hydrogen centre embedded in a Niobium crystal lattice is given. The electronic structure is investigated on the basis of a special energy difference procedure developed by Wahl et al. This procedure, here applied in its lowest approximation, yields the change in the electronic energy and electronic density distribution due to the embedded hydrogen atom. From these quantities, the dipole force tensor, the displacement of the ions close to the interstitial (nearest and next nearest neighbours) and the heat of solution are calculated. The computed results show good agreement with experimental data.

1. Introduction

Motivated by technical applications and physical aspects, metal hydride systems have been the subject of research since many years. This holds in particular for transition metal hydrides such as NbH_x, PdH_x and VaH_x, which exhibit a very high storage capacity. At present there is a great amount of experimental data at our disposal. On the other hand, a fundamental understanding of the nature of these systems is still in the beginning. This deficiency is mainly due to the complexity of the electronic interactions. Most studies on the behaviour of the interacting constituents (diffusion properties [1], phase transitions [2]) depend so far upon phenomenological model potentials.

Insight into the nature of the hydrogen-metal interaction has been obtained by considering a single impurity in the free electron gas [3–5]. During the last years a series of more sophisticated calculations could improve the quantitative understanding of this interaction. Nordlander et al. [6] have calculated heats of solution and lattice relaxations for several transition metal hydrides by replacing the real crystal by a physically representative effective medium for which calculations can be done in a self-consistent way. Differences between the true host and the effective medium are treated perturbatively. A review of further theoretical work concerning non-stoichiometric electronic problems in transition metal hydrides is given in [7].

Wahl et al. [8] have proposed a microscopic theory of metal hydride systems which is primarily based on first principles. Assuming a two-fold adiabatic approximation, the problem of calculating heats of solution is separated into three difference problems related to the energy change in the electronic, in the protonic and in the ionic subsystem. According to the hierarchy of coupling these subproblems must be solved succesively. Detailed investigations concern the computation of the electronic energy difference. This subtle task is mastered by a special field theoretical energy difference procedure developed by the authors on the fundaments of the New-Tamm-Dancoff method. Its essential point is a transformation of the difference problem to a functional eigenvalue problem in a suitably chosen tensor product space built up on a physical quasi-particle vacuum state. A detailed exposition of the formalism is given in [8] and [9–11] (mathematical foundations).

Based on Wahl et al.'s conception the paper in hand presents an approach to transition metal hydrides. Supposing a model of non-interacting hydrogen interstitials at low concentration we treat a single hydrogen centre in a Niobium host [12]. Principal subject is an investigation of the electronic configuration: the impurity induced change in the electron density and the electronic contribution to the heat of solution is evaluated in the lowest approximation of the energy difference procedure. Proton and ions are treated as classical particles, thermally induced movements are neglected. The effective ion-ion interaction is assumed to obey the harmonic approximation. Thus the total

---

* Supported by the Alfried Krupp von Bohlen and Halbach-Foundation.

Reprint requests to Prof. Dr. F. Wahl, Institut für Theoretische Physik, Universität Tübingen, Auf der Morgenstelle 14, D-7400 Tübingen 1.

0932-0784 / 88 / 1100-0914 $ 01.30/0. – Please order a reprint rather than making your own copy.

Dieses Werk wurde im Jahr 2013 vom Verlag Zeitschrift für Naturforschung in Zusammenarbeit mit der Max-Planck-Gesellschaft zur Förderung der Wissenschaften e.V. digitalisiert und unter folgender Lizenz veröffentlicht: Creative Commons Namensnennung-Keine Bearbeitung 3.0 Deutschland Lizenz.

Zum 01.01.2015 ist eine Anpassung der Lizenzbedingungen (Entfall der Creative Commons Lizenzbedingung „Keine Bearbeitung") beabsichtigt, um eine Nachnutzung auch im Rahmen zukünftiger wissenschaftlicher Nutzungsformen zu ermöglichen.

This work has been digitalized and published in 2013 by Verlag Zeitschrift für Naturforschung in cooperation with the Max Planck Society for the Advancement of Science under a Creative Commons Attribution-NoDerivs 3.0 Germany License.

On 01.01.2015 it is planned to change the License Conditions (the removal of the Creative Commons License condition "no derivative works"). This is to allow reuse in the area of future scientific usage.

heat of solution is calculated in dependence on the equilibrium position of the relaxed ions (nearest and next nearest neighbours). Minimizing this quantity yields the actual force pattern and the displacement field close to the perturbation centre.

2. Basic Conception

2.1 *Storage Energy*

As illustrated in Fig. 1 we introduce three reference systems:

(R1): the pure unperturbed host and outside the crystal a single hydrogen atom
(R2): the host deformed by Kanzaki forces
(R3): the host with the hydrogen atom inside

Let E_1, E_2, E_3 denote the total energy of the systems (R1), (R2), (R3), respectively.

We define the *storage energy* of the interstitially dissolved hydrogen atom by the energy difference between the hydrided system and the initial system, $E_3 - E_1$**. It is conveniently composed of an elastic part $E_2 - E_1$ and an impurity specific contribution $E_3 - E_2$. Writing down the first term in the harmonic approximation, the storage energy takes the form

$$\Delta E_{\mathrm{st}}(\boldsymbol{s}) = \tfrac{1}{2}\,\boldsymbol{s}\,\boldsymbol{\Phi}\,\boldsymbol{s} + Q(\boldsymbol{s}) - E_0 . \qquad (2.1)$$

$\boldsymbol{s} = (\ldots \boldsymbol{s}^n \ldots)$ denotes the ionic displacement field, $\boldsymbol{\Phi}$ the tensor of force constants. $Q(\boldsymbol{s})$ represents the interaction of the hydrogen centre with the components of the deformend host (R2). E_0 is the Coulomb energy of the isolated hydrogen atom (-13.6 eV).

Concerning the protonic and the ionic subsystems we employ a classical description. The particles are assumed to rest in their equilibrium positions, equivalent to the conditions at $T = 0$. On the basis of these approximations we can separate the Coulomb interaction between proton and ions:

$$Q(\boldsymbol{s}) = \sum_n \frac{Z e^2}{|\boldsymbol{X}^n - \boldsymbol{Y}|} + \omega(\boldsymbol{s}) . \qquad (2.2)$$

$\boldsymbol{X}^n$ and $\boldsymbol{Y}$ are the ionic and protonic coordinates, Z is the ionic charge; in accordance with the number of valence electrons in the niobium atom we set $Z = 5$.

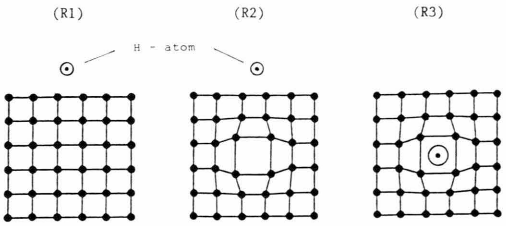

Fig. 1. Schematic illustration of the reference systems.

With regard to subsequent considerations, the proton-ion interaction potential is split into a contribution applying to the ideal lattice sites $\mathring{\boldsymbol{X}}^n$ and a difference term, including the displacements of the ions:

$$\sum_n \frac{Z e^2}{|\boldsymbol{X}^n - \boldsymbol{Y}|} = \sum_n \frac{Z e^2}{|\mathring{\boldsymbol{X}}^n - \boldsymbol{Y}|} + \underbrace{\sum_n \left(\frac{Z e^2}{|\mathring{\boldsymbol{X}}^n + \boldsymbol{s}^n - \boldsymbol{Y}|} - \frac{Z e^2}{|\mathring{\boldsymbol{X}}^n - \boldsymbol{Y}|} \right)}_{=: D_{\mathrm{p}}(\boldsymbol{s}) .} \qquad (2.3)$$

$\omega(\boldsymbol{s})$ represents the electronic contribution to the storage energy. More precisely: $\omega(\boldsymbol{s})$ corresponds to the energy difference between the electron systems of the reference systems (R3) and (R2). It is the exclusive contents of Chapt. 3 to discuss and compute this quantity.

2.2 *Force Pattern and Ionic Displacement Field*

We consider the concrete case of a hydrogen centre occupying a tetrahedral interstitial site in a bcc crystal lattice.

The equilibrium position of the neighbouring ions is determinated by the minimum of the storage energy

$$\nabla_{\boldsymbol{s}^m} \Delta E_{\mathrm{st}}(\boldsymbol{s})|_{\boldsymbol{s}} = 0 . \qquad (2.4)$$

Inserting (2.1) yields a force equation system:

$$-\nabla_{\boldsymbol{s}^m} Q(\boldsymbol{s})|_{\boldsymbol{s}} = \sum_n \Phi^{mn} \boldsymbol{s}^n . \qquad (2.5)$$

In the relaxed state the impurity induced (external) forces are compensated by the (internal) restoring forces of the lattice.

With the aid of the static lattice Green's tensor, (2.5) is resolved to the ionic displacements:

$$\boldsymbol{s}^m = -\sum_n G^{mn} \nabla_{\boldsymbol{s}^n} Q(\boldsymbol{s})|_{\boldsymbol{s}} . \qquad (2.6)$$

** This quantity differs from the experimentally observed heat of solution by half of the binding energy of the hydrogen molecule:

$$\Delta E_{\mathrm{st}} = \Delta H - 2.26\,\mathrm{eV}.$$

In our calculations external forces and ionic displacements are confined to the nearest and next nearest neighbours. Non radial components are neglected. On these conditions (2.6) reduces to a system of two coupled equations:

$$s^{\mathrm{I}} = f^{\mathrm{I}}(s^{\mathrm{I}}, s^{\mathrm{II}}) \cdot g^{\mathrm{I\,I}} + f^{\mathrm{II}}(s^{\mathrm{I}}, s^{\mathrm{II}}) \cdot g^{\mathrm{I\,II}}, \tag{2.7 a}$$

$$s^{\mathrm{II}} = f^{\mathrm{I}}(s^{\mathrm{I}}, s^{\mathrm{II}}) \cdot g^{\mathrm{II\,I}} + f^{\mathrm{II}}(s^{\mathrm{I}}, s^{\mathrm{II}}) \cdot g^{\mathrm{II\,II}}. \tag{2.7 b}$$

Here s^{I} and s^{II} denote the displacements of the first and second neighbours, and f^{I} and f^{II} the external forces on the ions. The terms $g^{\alpha\beta}$ describe the response (radial component) of the ions α to (radial) unit forces on the ions β. In detail:

$g^{\mathrm{I\,I}} := \langle \boldsymbol{e}^{\boldsymbol{m}} \mid \sum\limits_{\mathrm{n.\,n.}} G^{\boldsymbol{mn}} \boldsymbol{e}^{\boldsymbol{n}} \rangle$	$g^{\mathrm{II\,I}} := \langle \boldsymbol{e}^{\boldsymbol{m}} \mid \sum\limits_{\mathrm{n.\,n.}} G^{\boldsymbol{mn}} \boldsymbol{e}^{\boldsymbol{n}} \rangle$
$g^{\mathrm{I\,II}} := \langle \boldsymbol{e}^{\boldsymbol{m}} \mid \sum\limits_{\mathrm{n.\,n.\,n.}} G^{\boldsymbol{mn}} \boldsymbol{e}^{\boldsymbol{n}} \rangle$	$g^{\mathrm{II\,II}} := \langle \boldsymbol{e}^{\boldsymbol{m}} \mid \sum\limits_{\mathrm{n.\,n.\,n.}} G^{\boldsymbol{mn}} \boldsymbol{e}^{\boldsymbol{n}} \rangle$
$\boldsymbol{m}$ any nearest neighbour (n. n.)	$\boldsymbol{m}$ any next nearest neighbour (n. n. n.).

$\boldsymbol{e}^{\boldsymbol{m}}$: unity vector proton → ion $\boldsymbol{m}$ (non relaxed position).

The Green's tensor elements are taken from the compilation by Schober, Mostoller and Dederichs [13]. The computation of the solutions S^{I}, S^{II}* is performed by a suitable iteration procedure.

From the forces $F^{\mathrm{I}} := f^{\mathrm{I}}(S^{\mathrm{I}}, S^{\mathrm{II}})$, $F^{\mathrm{II}} := f^{\mathrm{II}}(S^{\mathrm{I}}, S^{\mathrm{II}})$ and the ideal lattice sites $\mathring{\boldsymbol{X}}^{\boldsymbol{n}}$ we obtain the elements of the dipole force tensor

$$P_{ij} := \sum_{\boldsymbol{n}} \mathring{X}_i^{\boldsymbol{n}} F_j^{\boldsymbol{n}}. \tag{2.8}$$

Owing to the symmetry of the interstitial sites, non diagonal elements vanish. In the case of an y-site we expect

$$\mathbf{P} = \begin{pmatrix} \mathrm{A} & 0 & 0 \\ 0 & \mathrm{B} & 0 \\ 0 & 0 & \mathrm{A} \end{pmatrix}. \tag{2.9}$$

In a finite crystal with a free surface, dipole force tensor and volume change are related by

$$\Delta V = \mathrm{Tr}\{\mathbf{P}\}/3\,K, \tag{2.10}$$

where K is the compressional or bulk modulus ($K = 1.73 \cdot 10^{12}\,\mathrm{dyn/cm^2}$ for niobium).

3. Electronic Part

3.1 *Formulation of an One Particle Problem*

We start from the many particle Schroedinger equations characterizing the electronic subsystems of the hydrided system (R3) and of the pure host (R2), respectively:

$$\text{(R3):}\quad \mathbf{H}_{\mathrm{H}}(\boldsymbol{x}, \boldsymbol{s})\, \Psi_{\mathrm{H}}(\boldsymbol{x}, \boldsymbol{s}) = E_{\mathrm{H}}(\boldsymbol{s})\, \Psi_{\mathrm{H}}(\boldsymbol{x}, \boldsymbol{s}), \tag{3.1 a}$$

$$\text{(R2):}\quad \mathbf{H}_{\mathrm{R}}(\boldsymbol{x}, \boldsymbol{s})\, \Psi_{\mathrm{R}}(\boldsymbol{x}, \boldsymbol{s}) = E_{\mathrm{R}}(\boldsymbol{s})\, \Psi_{\mathrm{R}}(\boldsymbol{x}, \boldsymbol{s}). \tag{3.1 b}$$

For the Hamiltonians $\mathbf{H}_{\mathrm{H}}$ and $\mathbf{H}_{\mathrm{R}}$ we refer to [8].

In the context of calculating heats of solution we are less interested in the absolute energy values E_{H} and E_{R}, but much more in the difference quantity

$$\omega(\boldsymbol{s}) := E_{\mathrm{H}}(\boldsymbol{s}) - E_{\mathrm{R}}(\boldsymbol{s}). \tag{3.2}$$

An appropriate tool to treat such energy differences exists in the procedure by Wahl et al. [8]. In its lowest approximation it is equivalent to a so-called rigid band model: The additional hydrogen electron is assumed to interact with crystal electrons which are frozen in the state corresponding to the unloaded host. The original many particle problem reduces thereby to the much simpler task of investigating the behaviour of a single electron in a rigid potential.

Concretely the formalism yields a non local one particle Schroedinger equation (equation (7.1) of [8]):

$$S_1(\boldsymbol{x}, \boldsymbol{x}')\,(\mathring{H}(\boldsymbol{x}') + P(\boldsymbol{x}') + D(\boldsymbol{x}'))\, S_1(\boldsymbol{x}', \boldsymbol{y})\, h(\boldsymbol{y}) = \lambda \cdot h(\boldsymbol{x}). \tag{3.3}$$

Here

$$\mathring{H}(\boldsymbol{x}) := -\frac{\hbar^2}{2m} - \sum_{\boldsymbol{n}} \frac{Z e^2}{|\boldsymbol{x} - \mathring{\boldsymbol{X}}^{\boldsymbol{n}}|} + \int_{\boldsymbol{z}} \frac{e^2\, \mathring{n}_{\mathrm{E}}(\boldsymbol{z})}{|\boldsymbol{x} - \boldsymbol{z}|}\, \mathrm{d}\boldsymbol{z} - 3\,e^2 \left(\frac{3}{8\,\pi}\right)^{1/3} \cdot \alpha \cdot \mathring{n}_{\mathrm{E}}(\boldsymbol{x})^{1/3} \tag{3.4}$$

represents the kinetic energy and the Hartree Fock interaction with the components of the unperturbed crystal. Diverging from [8], the original non local exchange potential is replaced by the Slater X_α-approximation ($\alpha = 0.8$, compare [14]);

$$P(\boldsymbol{x}) := -\,e^2 \frac{1}{|\boldsymbol{x} - \boldsymbol{Y}|} \tag{3.5}$$

contributes the Coulomb interaction with the embedded proton;

$$D(\boldsymbol{x}) \equiv D(\boldsymbol{x}, \boldsymbol{s}) := -\sum_{\boldsymbol{n}} \frac{Z e^2}{|\boldsymbol{x} - (\mathring{\boldsymbol{X}}^{\boldsymbol{n}} + \boldsymbol{s}^{\boldsymbol{n}})|} + \sum_{\boldsymbol{n}} \frac{Z e^2}{|\boldsymbol{x} - \mathring{\boldsymbol{X}}^{\boldsymbol{n}}|} \tag{3.6}$$

includes the displacements of the ions.

---

* Note: by the use of small and capital letters we distinguish between the parameters s^{I}, s^{II} and the realized dislocations S^{I}, S^{II}.

By the operators

$$S_1(\mathbf{x},\mathbf{x}') := \sum_{\mathbf{k}\ \text{unocc.}} \mathring{b}_{\mathbf{k}}(\mathbf{x})\, \mathring{b}^{*}_{\mathbf{k}}(\mathbf{x}') \tag{3.7}$$

the eigenfunction h is projected onto the unoccupied valence band states $\mathring{b}_{\mathbf{k}}$ of the ideal crystal. In other words: The state of the additional electron is orthogonalized to the occupied states of the valence band.

We obtain the total electronic energy difference by adding up the electron's energy eigenvalue λ and the energy contribution due to the interaction of the proton with the crystal electrons:

$$\omega := \lambda - \int_{\mathbf{x}} \frac{e^2\, \mathring{n}_{\mathrm{E}}(\mathbf{x})}{|\mathbf{x}-\mathbf{Y}|}\, \mathrm{d}\mathbf{x}. \tag{3.8}$$

Finally, the impurity induced change in the electron density is given by the absolut square of the eigenfunction:

$$\Delta\varrho(\mathbf{x}) = |h(\mathbf{x})|^2. \tag{3.9}$$

We return to the one particle equation (3.3). On looking more carefully, it reveals some crucial inadequacies:

> Whereas the ionic displacements enter by the difference term $D(\mathbf{x},\mathbf{s})$, the electron system is represented by the density function $\mathring{n}_{\mathrm{E}}(\mathbf{x})$ and the Bloch waves $\mathring{b}_{\mathbf{k}}(\mathbf{x})$, which refer both to the ideal crystal.
> The ionic interaction is characterized by pure Coulomb potentials. These leave out of account that ions are spatially extended particles composed of a core and of core electrons. In particular there is no orthogonalization to the core electron states.

Supplementary correction terms will remove these deficiencies.

3.2 Treatment of the One Particle Equation

A) Orthogonalization to the Host's Electron States

Niobium is a transition metal characterized by the atomic electron configuration $(4\,\mathrm{s})^4\,(5\,\mathrm{s})^1$.

The gradually filled d-shell in the atom and the small energy difference separating the 4d- and 5s-niveaus results in a band structure in the crystal which is typical for transition metals: s- and d-band overlap, the d-band extends through the Fermi energy. Whereas the electrons of the s-band can be regarded as collective electrons, the d-band states still show atomic character and the corresponding electrons are tied to the ions. Thus these metals exhibit a very complex and manifold structured Fermi surface, quite unlike the slightly deformed free electron spheres of simple metals.

The complexity of the Bloch states and of the Fermi surface renders a realistic description of the S_1-projectors very difficult. To avoid numerical excesses we deviate from the original formulation and proceed as follows:

In a first step the projectors are altered to produce orthogonality exclusively to the 5s-valence band states. Approximating these states by plane waves, the projectors reduce to the form

$$\begin{aligned} S_1(\mathbf{x},\mathbf{x}') &= \frac{1}{\Omega} \sum_{k>k_{\mathrm{F}}} e^{i\mathbf{k}(\mathbf{x}-\mathbf{x}')} \\ &\simeq \frac{1}{8\pi^3} \int_{k>k_{\mathrm{F}}} e^{i\mathbf{k}(\mathbf{x}-\mathbf{x}')}\, \mathrm{d}\mathbf{k}, \end{aligned} \tag{3.10}$$

where the Fermi radius k_{F} corresponds to one valence electron per ion.

A second step takes care of the localized electrons: Following the idea of the pseudopotential method, we simulate orthogonality to the core states and 4d-valence band states by additional repulsion effects in the vicinity of the ions. These are realized by attaching to each of the ions a hardcore potential

$$V_{\mathrm{hc}}(x) := \frac{Z e^2}{x}\, e^{-\gamma x^2}, \tag{3.11}$$

where γ is restricted to the range $0.4 \leqq \gamma \leqq 0.5$.

Together with the bare Coulomb potential it constitutes an effective ion potential

$$V_{\mathrm{eff}}^{\mathrm{ion}}(x) := -\frac{Z e^2}{x}\,(1 - e^{-\gamma x^2}). \tag{3.12}$$

Figure 2 illustrates these potentials for $\gamma = 0.4$ and $\gamma = 0.5$.

The hardcore ansatz draws inspiration from the pseudopotential given by Ho et al. [14] (see appendix). This semi-local potential, established for band structure calculations in bulk Niobium, indicates a strong core repulsion to the s- and p-component of the wave function and a much weaker repulsion to the d-component (Figure 6). We have chosen an effective potential comparable to the local components V_{s} and V_{p} of that pseudopotential. This ensures an adequate description of the core state orthogonality and includes at least qualitative aspects of an orthogonalization to the 4d-valence band states.

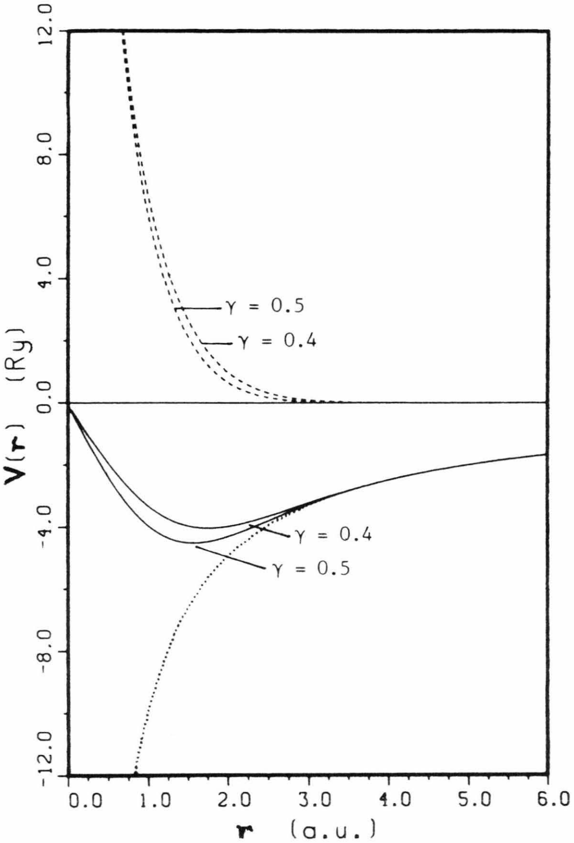

Fig. 2. Coulomb potential (dotted line), hardcore potential (dashed lines) and effective potential (solid lines) for $\gamma = 0.4$ and $\gamma = 0.5$.

From the effective potentials of the individual ions we obtain the effective ion potential of the crystal

$$V_{\text{eff}}(\boldsymbol{x}) := \sum_{\boldsymbol{n}} V_{\text{eff}}^{\text{ion}}(\boldsymbol{x} - \mathring{\boldsymbol{X}}^{\boldsymbol{n}}). \tag{3.13}$$

B) *Valence Electron Density and Hartree Fock Potential*

The valence charge distribution of the unperturbed niobium crystal is available from the calculations of Ho et al. [14]. Their paper presents contour plots which provide sufficient information to reproduce the charge distribution $\mathring{n}_{\text{E}}(\boldsymbol{x})$ in the whole space. The density is zero in the centre of the ions and then rises up sharply to form lobes with distinct d-like character around the ions. In addition to the lobes, there is a uniform charge background in the interionic space.

We employ this valence electron density to built up the Hartree potential and the exchange potential (second and third potential terms in (3.4)). With the effective ion potential they combine to the potential of the unrelaxed crystal. The latter is shown in Fig. 3 (dashed curve) along the line proton ↔ first neighbour ion. The plot indicates a flat potential plateau in the space between the ions and a distinct potential peak around the ions. The solid curve represents the total potential, including the crystal potential and the protonic Coulomb potential.

Figure 4 illustrates the potential uncertainty involved by the hardcore parameter. At the same time it

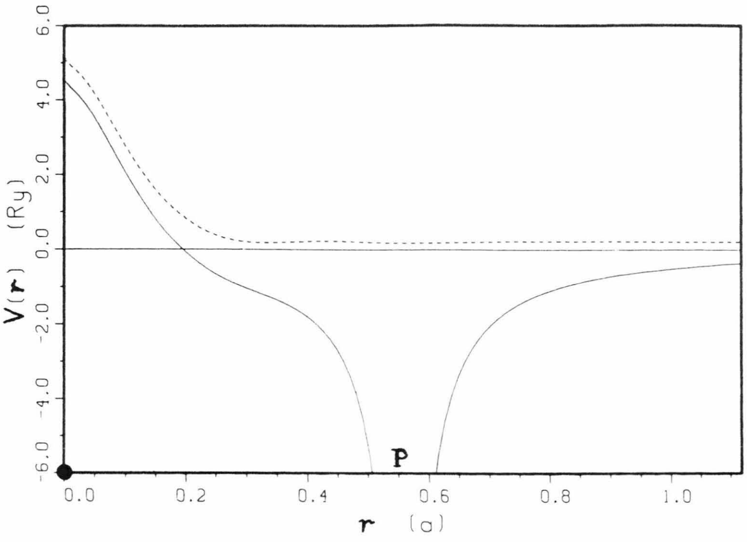

Fig. 3. The crystal potential (dashed curve) and the total potential (solid curve) along the line proton (P) ↔ first neighbour ion (●).

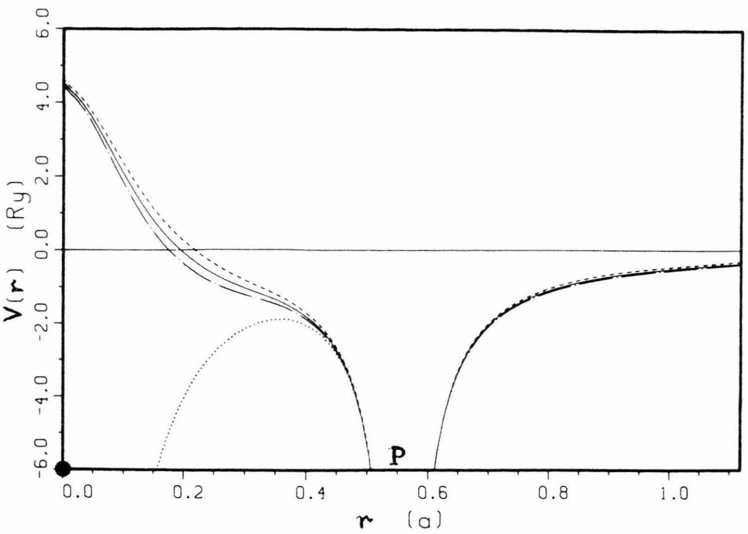

Fig. 4. The total potential for different values of the hardcore parameter: $\gamma = 0.4$ (dashed curve), $\gamma = 0.45$ (solid curve) and $\gamma = 0.5$ (dash dotted curve); the dotted curve shows the potential, when no hardcore repulsion is included.

demonstrates the importance of including core state orthogonalization: Without a hardcore barrier, the hydrogen electron could penetrate into the ions and would drop into the funnel of the dominant ionic Coulomb potential (dotted line).

C) Difference Potential

We have already pointed to a problem concerning the description of the crystal relaxation: Our formalism considers displacements of the ions, but it takes no account of a corresponding change in the valence electron system. A modified difference potential compensates for this deficiency:

We assume that the dislocation of an ion causes an equivalent shift of the accompanying 4d-valence electrons. To adapt the hardcore potential to the shifted electron states (core states and 4d-valence band states), the Coulomb potentials in the ionic difference term (3.6) are replaced by the effective ion potentials. Moreover the relaxed valence electron density will screen the ionic difference term. This effect is simulated by a reduced ion charge Z_r. Corresponding to the shifted net charge, we set $Z_r = 1$. In this way we obtain a weak difference potential

$$\begin{aligned}\tilde{D}(x, s) &:= \frac{Z_r}{Z}\left(V_{\text{eff}}(x, X) - V_{\text{eff}}(x, \mathring{X})\right) \\ &= -\sum_n Z_r e^2 \frac{1 - e^{-\gamma(x - X^n)^2}}{|x - X^n|} \\ &\quad + \sum_n Z_r e^2 \frac{1 - e^{-\gamma(x - \mathring{X}^n)^2}}{|x - \mathring{X}^n|}. \qquad (3.14)\end{aligned}$$

Analogously we deal with the difference term connected to the proton-ion interaction (see (2.2), (2.3) and (3.8)). It is replaced by the screened version

$$\tilde{D}_p(x, s) := \frac{Z_r}{Z} D_p(x, s). \qquad (3.15)$$

3.3 Basis Functions

We expect an eigenfunction well localized about the proton. A subtle task consists in the choice of an adequate basis system: on the one hand, this set should be approximately complete in the region of interest, on the other hand the number of basis functions should be small to keep the calculations tractable.

It has appeared that the hydrogen functions Φ^z_{nlm}* do not work satisfactorily. They fail in producing the required orthogonality to the free electron states of the 5s-valence band. An appreciable improvement in convergence is achieved by using not simple hydrogen functions, but *orthogonalized hydrogen functions*

$$\Psi^z_{nlm}(x) := S_1(x, x')\, \Phi^z_{nlm}(x') \qquad (3.16)$$

which are orthogonal to the 5s-states right from the start.

---

* We mean the eigenfunctions of the equation $\left(p^2/2m - \frac{z}{x}\right)\phi(x) = E\,\phi(x)$.

		Calculated values			Experimental dates
		$\gamma = 0.5$	$\gamma = 0.45$	$\gamma = 0.4$	
ionic displacements [Å]	S^{I}	0.0974	0.1027	0.1108	0.10
	S^{II}	0.0139	0.0119	0.0096	0.008
external forces [eV/Å]	F^{I}	0.9519	0.9997	1.0743	1.0
	F^{II}	0.2320	0.2274	0.2244	0.23
elements of the dipol force tensor [eV]	A	3.234	3.367	3.581	3.37
	B	3.365	3.348	3.434	3.37
volume change per unity cell	$\Delta V/V_0$	0.1681	0.1732	0.1821	0.175
storage energy [eV]	ΔE_{sp}	−3.512	−2.570	−1.306	−2.59

Table 1. A compilation of calculated results and experimental data. Excepted for the storage energy which is taken from McLellan and Harkins [16], the experimental values are based on X-ray studies by Peisl [15].

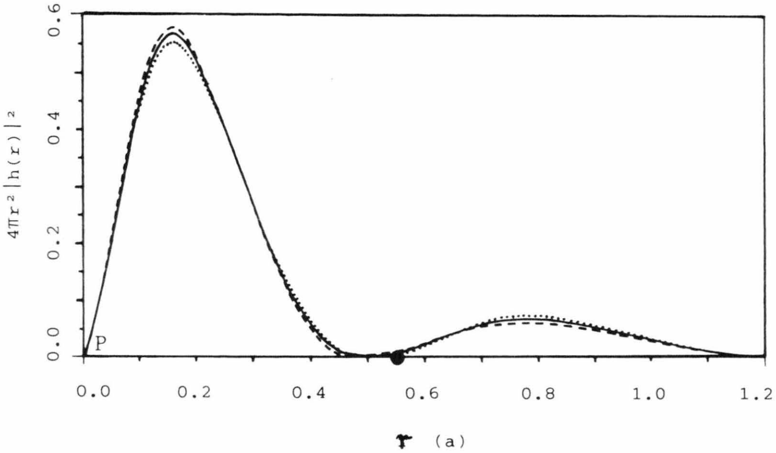

Fig. 5. The function $4\pi r^2 |h(\boldsymbol{r})|^2$ in the direction proton (P) ↔ first neighbour ion (●) for $\gamma = 0.4$ (dashed line), $\gamma = 0.45$ (solid line) and $\gamma = 0.5$ (dotted line).

An appropriate expansion of the eigenfunction is given by

$$h(\boldsymbol{x}) = \beta^{1\cdot}_{100}\,\Psi^{1\cdot}_{100}(\boldsymbol{x}) + \sum_{n=1}^{7}\ \sum_{l=0}^{\min(n-1,l)}\ \sum_{m=-l}^{l} \beta^{5\cdot}_{nlm}\,\Psi^{5\cdot}_{nlm}(\boldsymbol{x}). \tag{3.17}$$

This ansatz is substantiated in detail in [12].

Proceeding from the expansion (3.17) we compute the matrix elements

$$M\begin{pmatrix} n_2, l_2, m_2, z_2 \\ n_1, l_1, m_1, z_1 \end{pmatrix} := \langle \Psi^{z_2}_{n_2, l_2, m_2} | H + P + D | \Psi^{z_2}_{n_1, l_1, m_1} \rangle$$

and

$$U\begin{pmatrix} n_2, l_2, m_2, z_2 \\ n_1, l_1, m_1, z_1 \end{pmatrix} := \langle \Psi^{z_2}_{n_2, l_2, m_2} | \Psi^{z_1}_{n_1, l_1, m_1} \rangle$$

to determine subsequently the eigenvalue λ and the coefficients β^z_{nlm} (dependent on the displacements s^{I} and s^{II}) from the eigenvalue problem

$$\mathbf{M}\,\boldsymbol{\beta} = \lambda\,\mathbf{U}\,\boldsymbol{\beta}. \tag{3.18}$$

4. Results

Numerical calculations have been performed for different values of the hardcore parameter, namely $\gamma = 0.4$, $\gamma = 0.45$ and $\gamma = 0.5$.

We obtain a well localized and almost radially symmetric eigenfunction $h(\boldsymbol{r})$. Figure 5 shows the corresponding density function $4\pi r^2 |h(\boldsymbol{r})|^2$** from the proton in the direction of a first neighbour ion. It is characterized by a principal peak at a distance of ca. 0.2 lattice constants from the impurity centre, followed by a series of descending secondary peaks, each separated by a zero level.

The results for the lattice expansion, the external forces and the storage energy are presented in Table 1,

---

** Because of the approximate radial symmetry of the eigenfunction, the function $4\pi r^2 \cdot |h(\boldsymbol{r})|^2$ (drawn in a certain direction) is a reasonable approach to the *radial density distribution* of the additional electron.

together with experimental data. This compilation shows some interesting features:

(i) except for the displacement of the next nearest neighbours, the experimental values are located within the range tolerated by the calculations;

(ii) in particular there is an excellent agreement between the experimental data and the results achieved by the $\gamma = 0.45$ computation;

(iii) the storage energy appears to be very sensitive to a variation of the hardcore parameter.

Let us try a concluding valuation of our model on the basis of the results presented above. Treating the electronic problem, we have used the energy difference procedure in its lowest approximation. The density change in the electron system is given there by the absolute square of the one particle state function, $\Delta\varrho(\mathbf{r}) = |h(\mathbf{r})|^2$. This excludes a description of Friedel oscillations, as they are typical for a screened proton, from the beginning. Yet we know from the investigations of Göbel and Wahl ([17], [18]), that an inclusion of higher order terms in the difference procedure would actually produce oscillations round the zero level.

Unfortunately the uncertainty in the hardcore potential prevents a determination of the storage energy with a sufficient accuracy. To illuminate the sensitivity of this quantity to the choice of the hardcore parameter, we consider again the effective ion potentials drawn in Figure 4. Though quite similar in their shape, the $\gamma = 0.4$- and the $\gamma = 0.5$-curves show absolute potential differences up to 0.7 Ry $\simeq$ 9.5 eV at a distance of 0.2 lattice constants from the ion. As the eigenfunction extends into these regions, a distinct energy difference in the corresponding eigenvalues and consequently in the storage energies (ca. 2.2 eV) is not astonishing. These facts demonstrate the necessity of a very accurate knowledge of the crystal potential.

A delicate approximation consists further in the primitive screening of the difference potentials by a multiplication factor $Z_r/Z = 1/5$. The excellent results obtained for the lattice expansion and the corresponding external forces prove that this approximation is not as bad as it is simple.

The present work marks the start of a series of investigations concerning niobium hydride. So we have already treated the proton quantum mechanically in order to determine local excitation energies. First results are presented in [19]. Furthermore we have developed a model of two interacting impurity centres. On this topic a publication is in preparation.

Appendix

The Pseudopotential of Ho et al.

Using the pseudopotential method, Ho, Louie, Chelikowsky, and Cohen have calculated the electronic structure of bulk niobium [14]. Their approach is based on a pseudopotential Hamiltonian

$$H := p^2/2m + V_{\mathrm{ps}} + V_{\mathrm{H}} + V_x, \tag{A.1}$$

where the electron-ion interaction is realized by a weak pseudopotential

$$V_{\mathrm{ps}}(\mathbf{x}) := \sum_{\mathbf{n}} V_{\mathrm{ps}}^{\mathrm{ion}}(\mathbf{x} - \mathring{\mathbf{X}}^{\mathbf{n}}) \tag{A.2}$$

with

$$V_{\mathrm{ps}}^{\mathrm{ion}}(\mathbf{x}) := \sum_{l} V_l(x)\, P_l. \tag{A.3}$$

P_l is a projection operator acting on the lth angular momentum component of the wave function. The local potentials V_l (Fig. 6) take into account the Coulomb potential as well as the repulsion that each angular momentum sees as a result of the core orthogonalization.

The ionic pseudopotential is screened by adding a Hartree potential and a local Slater X_α-exchange potential V_x ($\alpha = 0.8$).

Acknowledgement

It is a pleasure for K. Hau and P. Frodl to acknowledge the Alfried Krupp von Bohlen and Halbach-foundation for financial support.

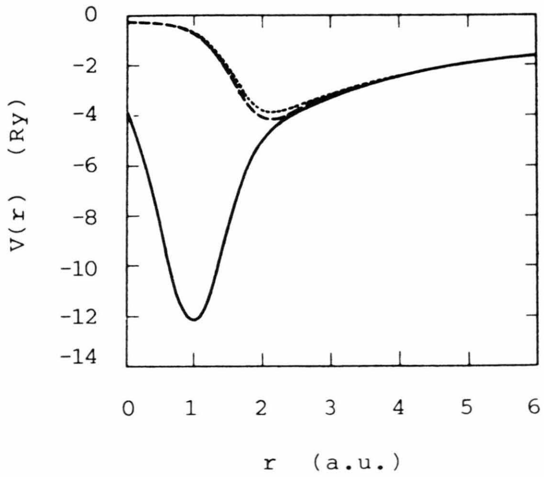

Fig. 6. Nb^{+5} ionic pseudopotentials V_s (dashed line), V_p (dotted line) and V_d (solid line) plotted as a function of r.

[1] H. Teichler and A. Klamt, Phys. Lett. **108 A,** 281 (1985).
[2] C. K. Hall, Electronic Structure and Properties of Hydrogen in Metals, Plenum Press N.Y., 11 (1983).
[3] P. Jena and K. S. Singwi, Phys. Rev. **B17,** 3518 (1978).
[4] J. K. Nørskov, Phys. Rev. **B 20,** 446 (1979).
[5] B. Gumhalter and V. Zlatić, J. Phys. **C13,** 1679 (1980).
[6] P. Nordlander, J. K. Nørskov and F. Besenbacher, J. Phys. **F16,** 1161 (1986).
[7] A. Bansil, R. Prasad, and L. Schwarz, Electronic Structure and Properties of Hydrogen in Metals, Plenum Press N.Y. 249 (1983).
[8] F. Wahl, R. Duscher, K. Göbel, and J. Maichle, Z. Naturforsch. **39 a,** 524 (1984).
[9] W. Feist, Z. Naturforsch. **36 a,** 421 (1981).
[10] F. Wahl and W. Feist, Z. Naturforsch. **36 a,** 429 (1981).
[11] E. E. Müller and W. Feist, Z. Naturforsch. **38 a,** 1276 (1983).
[12] K. Hau, Ein Wasserstoffzentrum in Niob: Elektronenstruktur und Gitterstatik, Thesis, Tübingen 1987.
[13] H. R. Schober, M. Mostoller, and P. H. Dederichs, Phys. Stat. Sol. **B 64,** 173 (1974).
[14] K. M. Ho, S. G. Louie, J. R. Chelikowsky, and M. L. Cohen, Phys. Rev. **B15,** 1755 (1977).
[15] H. Peisl, X-Ray Studies of Interstitials in Metals, Proceedings of the Yamada Conference V, Kyoto 1982, North Holland Publ. Comp. 1982.
[16] R. B. McLellan and C. G. Harkins, Materials Science and Engineering **18,** 5 (1975).
[17] K. Göbel and F. Wahl, Z. Naturforsch. **41 a,** 1381 (1986).
[18] K. Göbel and F. Wahl, Z. Naturforsch. **42 a,** 431 (1987).
[19] F. Sommer, K. Hau, P. Frodl, and F. Wahl, Z. Naturforsch. **43 a,** 923 (1988).